LANGMUIR

pubs.acs.org/Langmuir Article

Combinatorial Analysis of Sparse Experiments on Photocatalytic Performance of Cement Composites: A Route toward Optimizing Multifunctional Materials for Water Purification

Pamela Zuniga Fallas, Jaime Quesada Kimzey, Prabhas Hundi, Md Tariqul Islam, Juan C. Noveron, Pedro J. J. Alvarez,* and Rouzbeh Shahsavari*

Cite This: *Langmuir* 2021, 37, 5699−5706 Read Online

ACCESS | Metrics & More | Article Recommendations | Supporting Information

ABSTRACT: Blending TiO_2 and cement to create photocatalytic composites holds promise for low-cost, durable water treatment. However, the efficiency of such composites hinges on cross-effects of several parameters such as cement composition, type of photocatalyst, and microstructure, which are poorly understood and require extensive combinatorial tests to discern. Here, we report a new combinatorial data science approach to understand the influence of various photocatalytic cement composites based on limited datasets. Using P25 nanoparticles and submicron-sized anatase as representative TiO_2 photocatalysts and methyl orange and 1,4-dioxane as target organic pollutants, we demonstrate that the cement composition is a more influential factor on photocatalytic activity than the cement microstructure and TiO_2 type and particle size. Among the various cement constituents, belite and ferrite had strong inverse correlation with photocatalytic activity, while natural rutile had a positive correlation, which suggests optimization opportunities by manipulating the cement composition. These results were discerned by screening 7806 combinatorial functions that capture cross-effects of multiple compositional phases and obtaining correlation scores. We also report •OH radical generation, cement aging effects, TiO_2 leaching, and strategies to regenerate photocatalytic surfaces for reuse. This work provides several nonintuitive correlations and insights on the effect of cement composition and structure on performance, thus advancing our knowledge on development of scalable photocatalytic materials for drinking water treatment in rural and resource-limited areas.

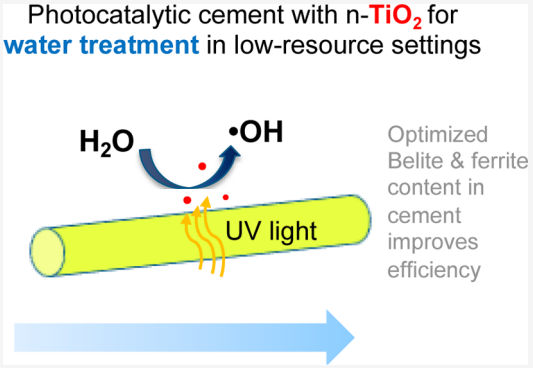

INTRODUCTION

Titanium dioxide (TiO_2) is a widely used semiconductor material with a wide range of applications in photocatalysis, heterogeneous catalysis, dye-sensitized solar cells, gas sensors, and corrosion protection.[1] While photocatalytic TiO_2 nanoparticles ($nTiO_2$) have been used in water purification,[2,3] their use in water treatment as a slurry/suspension requires energy-intensive separation processes—such as ultrafiltration—to enable reuse and prevent release into the treated water. This increases process complexity and operating cost,[4] hindering their commercial deployment and applications. Immobilization of $nTiO_2$ on solid supports such as alumina, silica, iron oxide, biopolymers, and concrete provides an opportunity to side-step this challenge.[5−7]

Among the various support materials, concrete holds great promise for enabling development of scalable photocatalytic water purification systems due to its low cost, abundance, and durability. Indeed, concrete is the most widely used synthetic material on the planet.[8] Common infrastructures such as parking slabs, Bayous, canals, and roads made of concrete could be designed to be photocatalytic, besides their mechanical functionalities. The key structural binder of concrete that immobilizes TiO_2 is cement. Although a number of previous reports have studied the mechanical and photocatalytic performance of cement composites containing $nTiO_2$,[9−13] majority of these studies focused on self-cleaning and air pollution-control properties.[14−16] Photocatalytic cement has been considered for oxidation of dyes from colored wastewaters by using distinct commercial cement types containing TiO_2 coatings.[17,18] However, adding TiO_2 on hardened cement could result in leaching of TiO_2 submicron particles in treated drinking water and eventual depletion of intended photocatalytic activity. An alternative approach to overcome this challenge is to prepare TiO_2−cement composites as a blend that firmly immobilizes the photocatalyst. This strategy not only yields more integrated

Received: March 8, 2021
Revised: April 11, 2021
Published: April 26, 2021

https://doi.org/10.1021/acs.langmuir.1c00654
Langmuir 2021, 37, 5699−5706

Table 1. Mineralogical Analysis of Different Anhydrous Neat Cement (Unamended with TiO_2) Powders (%)

cement	alite	belite	ferrite	calcite	lime	TiO_2 (rutile)	Al_2O_3	$AlPO_4$	Al_2TiO_5
WPC	23.5 ± 4	18.2 ± 15	3.1 ± 4	25.5 ± 10	23 ± 2	0.6 ± 3	6.4 ± 5		
OPC	31.8 ± 4	42 ± 4	10.9 ± 4	7.7 ± 5		0.1 ± 2	7.6 ± 9		
PPC	30.9 ± 5	28 ± 4	10.4 ± 7	6.7 ± 6		0.5 ± 2	2 ± 4	1.7 ± 3	9.1 ± 4
PPC-2	41.0 ± 4	10.5 ± 14	3.2 ± 8	0.0 ± 5		0.0	42.0 ± 3		

composites and minimizes leaching but also provides an expanded photoactive mass that can be accessible repeatedly, for example, by sanding off passivated surfaces, thereby regenerating photocatalytic activity.

Effective engineering and implementation of photocatalytic cements for water treatment require a thorough understanding of how several interrelated parameters affect composite performance and sustained reactivity. These parameters, whose interactive effects are poorly understood, include cement composition, cement microstructure, and type and particle size of TiO_2. Discerning the influence of such system properties and their interactive effects requires combinatorial experiments. Herein, we develop a new combinatorial data science approach to understand the influence of various photocatalytic cement constituents and properties based on limited datasets. We present a comprehensive report on the synthesis, characterization, and analysis of various photocatalytically active TiO_2–cement composites, decoding the influence of aforesaid parameters on the degradation of two dissimilar organic pollutants: methyl orange (MO), which is a mutagenic industrial (anionic) dye, and 1,4-dioxane, which is a potentially carcinogenic and highly recalcitrant industrial solvent frequently detected in drinking water sources.[19−21] We identify the key compositional parameters and mechanisms that enhance or inhibit the photocatalytic activity of TiO_2–cement composites, providing performance guidelines that can facilitate predictive design of TiO_2–cement composites.

EXPERIMENTAL SECTION

Basic Material Procurement and Characterizations. Four different commercial formulations of Portland cement were amended with TiO_2 to produce photoactive cementitious materials. Ordinary Portland cement (OPC) and two Pozzolanic-based Portland cements (PPC and PPC-2) were obtained from Holcim Ltd, while white Portland cement (WPC) was obtained from Cemex Materials LLC (Table 1). We also considered a commercial photoactive cement (PHC) designed for air purification obtained from Italcementi Group. Two photocatalysts (*i.e.*, anatase TiO_2 and P25 $nTiO_2$) obtained from Fisher Scientific and Evonik were used without further treatment.

Quantitative mineralogical analysis of OPC, PPC, PPC-2, and WPC was performed by the Rietveld method using powder X-ray diffraction (XRD). Surface areas of the photocatalysts were determined from N_2-adsorption experiments using Brunauer–Emmett–Teller (BET) surface area analysis (Quantachrome Autosorb-3b BET surface analyzer). XRD patterns obtained using a Rigaku SmartLab X-ray diffractometer identified the crystalline phases of TiO_2. Transmission electron microscopy (TEM, JEOL JM-2100 Plus) imaging and dynamic light scattering (DLS, Malvern Zen 3600) characterized the primary particle sizes of TiO_2.

Preparation and Characterization of Photocatalytic $nTiO_2$–Cement Composite Plates. Cement hydrate plates (diameter: 50 mm, thickness: 10 mm), hereto called cement plates, were prepared using the four cement formulations (OPC, PPC, PPC-2, and WPC) and two photocatalyst amendments (Evonik P25 $nTiO_2$ or anatase TiO_2). Unamended neat cement plates (no added TiO_2) were also prepared as negative controls. For 1,4-dioxane degradation experiments, a positive control was prepared with PHC for benchmarking. For all TiO_2–cement hydrate composites (hereto called TiO_2–cement composites), cement and TiO_2 were thoroughly dry mixed using 5 wt % TiO_2. A minimum amount of ultrapure water (UPW) was added to obtain a workable photoactive mixture (water/cement ratio of 0.3–0.5), which was then poured into plastic Petri dishes as molds for making TiO_2–cement plates, followed by curing for 24 h at room temperature. After curing, the plates were dried under ambient conditions and transferred to new Petri dishes for housing during performance tests. Scanning electron microscopy (SEM, FEI ESEM Quanta 600 FEG) and wavelength-dispersive spectroscopy (WDS) mapped titanium distribution on the TiO_2–cement composites.

Photocatalytic Degradation of MO and 1,4-Dioxane Using TiO_2–Cement Composites. Given that TiO_2 exhibits a negative charge at the alkaline pH[22] of cement, we tested the photocatalytic activity for water treatment using MO, a recalcitrant anionic dye, because of its azo and quinoid structures,[18] which exhibits minimum adsorption affinity toward the cement plates due to electrostatic repulsion. Photocatalytic degradation of 1,4-dioxane in water was also tested because it is a contaminant of emerging concern (due to its potential carcinogenicity and widespread occurrence in drinking water sources) that is commonly treated by advanced oxidation processes.[19−21,23]

To measure photocatalytic degradation, 6 mL of aqueous solution was poured on top of each TiO_2–cement composite plate (preparation described above). A layer of approximately 4 mm of MO (16 mg/L, 48.8 μM) or 1,4-dioxane solution in water (1 mL/L) was formed on the top of each TiO_2–cement plate. Identical Petri dishes containing only the solutions were considered as photolysis and evaporation controls. Next, the TiO_2–cement plates were exposed to UVC irradiation (254 nm) or lack thereof (for sorption tests) using a LZC-4 benchtop photoreactor for 30 min. Similarly, low UVC irradiation[24] (2.7 ± 0.4 mW/cm^2, distance between lamp and samples: 19.1 cm) was used to prevent sample evaporation in bench-scale photoreactors.[17] Additionally, low UVC irradiation decreases energy consumption and enhances the cost-effectiveness of photocatalytic water treatment. Following the 30 min UVC exposure, samples of the residual concentrations of MO and 1,4-dioxane solutions were measured by absorbance spectrophotometry (SpectraMax Plus from Molecular Devices) using a peak of absorbance at 480 nm and by a frozen micro-extraction/gas chromatography–mass spectrometry method,[25] respectively. MO and 1,4-dioxane experiments were done in quintuplicate and triplicate, respectively. Immediately after each experiment, the TiO_2–cement plates were wet-rubbed using a 3M 400-grit flexible diamond sand paper to regenerate the photoactive surface of the TiO_2–cement plates (hereafter called regeneration treatment).

Photocatalytic Generation of Hydroxyl Radicals ($^{\bullet}$OH) and Aging. Aging batch tests were designed to mimic conditions in drinking water storage tanks and discern inefficient commercial cement formulations that can compromise composite durability and its photocatalytic longevity. Aging tests were performed for 168 h (7 days) with UPW at 25° C. Cement plates were immerged in a 250 mL beaker filled with UPW, and every 24 h, the UPW was replaced. Aging of photocatalytic cements was characterized by their decreasing ability to generate $^{\bullet}$OH in aqueous solution over time, which is important to assess the required regeneration frequency. The terephthalic acid-mediated photoluminescence probe method[26] was used to measure photocatalytic hydroxyl radical ($^{\bullet}$OH) generation activity of the TiO_2–cement composites. The terephthalate solution was prepared by reacting terephthalic acid with stoichiometric amounts of NaOH. After 30 min of UVC light irradiation, the fluorescence emission spectra were taken on the resulting terephthalate solution, followed by

https://doi.org/10.1021/acs.langmuir.1c00654
Langmuir 2021, 37, 5699−5706

measuring the fluorescence intensity at 425 nm to assess •OH generation. Aging experiments were done in triplicate following the same procedures used for degradation of MO and 1,4-dioxane. The TiO_2−cement plates were tested after aging and after regeneration treatment.

RESULTS AND DISCUSSION

Structural and Chemical Characterization of Cements and Photocatalysts. The compositions of the commercial cement formulations are compared in Table 1. Major differences were found in the fraction of the natural key ingredients of cement such as alite, belite, ferrite, and calcite as well as minor constituents such as rutile TiO_2 and Al_2O_3 (Table 1). Table 2 shows the physical properties of the photocatalysts such as their crystalline phase, surface area, and particle size. The P25 $nTiO_2$ sample showed higher surface area than anatase TiO_2, consistent with the smaller size of P25 $nTiO_2$ measured *via* TEM and DLS. In our synthesis of the TiO_2−cement composites, the applied design parameters (*i.e.*, the lowest water−cement ratio and a curing time of 24 h at room temperature) favored obtaining cement structures that exhibited high strength and decreased porosity, in line with previous reports.[27,28]

Table 2. Characterization of $nTiO_2$ as Used for Cement Amendment[a]

sample	crystalline phase[a]	surface area[a] (m^2/g)	TEM mean size[b] (nm)
anatase	99.9% anatase	22.3 ± 4.7	167.5 ± 13.2
P25 (Evonik)	79% anatase 21% rutile	64.5 ± 5.5	37.5 ± 20.2

[a]Note: The physical properties of the photocatalyst could not be measured in the cement matrix. Therefore, the photocatalysts were characterized as used for cement amendment: (a) dry powder samples; (b) in aqueous suspension using UPW.

Photocatalytic Removal of MO: Role of TiO_2 Type Versus Cement Composition. Figure 1 shows the results of the photocatalytic degradation of MO by nine TiO_2−cement composites; that is, three cement types × three TiO_2 types (P25, anatase, and control). MO photocatalytic removal efficiencies after 30 min of treatment varied from 11.1% with OPC to 47.0% with WPC (after correction for sorption, Figure 2). Removal efficiency was affected by the cement composition, the type of TiO_2 added, and the embedded concentration of natural titanium content in cement. Several observations deserve attention here. First, addition of 5% (by weight) P25 $nTiO_2$ significantly improved photocatalytic activity with UVC-irradiated WPC and (to a lesser extent) PPC but not with OPC (Figure 1). This suggests that the composition of OPC (the most common type of cement) per se and/or the resulting hydrated microstructure of OPC are unsuitable for photocatalytic use as it was not improved by P25 $nTiO_2$ or anatase addition. Thus, OPC-based formulations should be avoided for preparing photocatalytic cement composites.

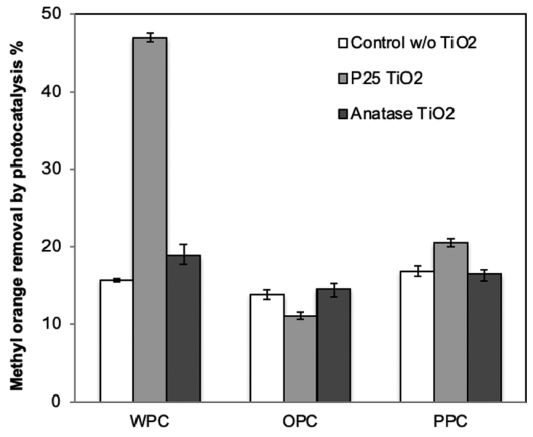

Figure 1. Photocatalytic removal of MO (corrected for sorption) by WPC, OPC, and PPC amended with TiO_2 (5% by weight). Error bars represent ± 1 standard deviation from the mean of all measurements. Test conditions were as follows: n = 5, exposure time: 30 min, pH = 10.53 ± 0.25, initial dye concentration: 16 mg/L, λ of ∼254 nm, light intensity: 2.7 ± 0.4 mW/cm.^{2}.

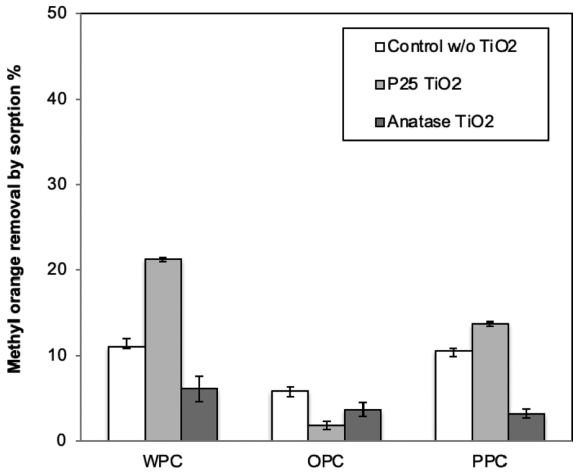

Figure 2. Sorptive removal of MO by WPC, OPC, and PPC amended with TiO_2 (5% by weight). Error bars represent ± 1 standard deviation from the mean of all measurements. Test conditions were as follows: n = 5, exposure time: 30 min in the dark, pH = 10.24 ± 0.25, initial dye concentration: 16 mg/L.

Both WPC and PPC exhibited higher photocatalytic removal efficiency when amended with P25 $nTiO_2$ (which consists of 79% anatase and 21% rutile, Table 2) than with anatase TiO_2, which in fact only improved the photocatalytic performance of WPC. This is most likely because of synergistic interactions between anatase and rutile in P25 $nTiO_2$, which increases activity; whereas the small band-structure differences between the TiO_2 polymorphs reduce energy levels of the rutile conduction band to lower-energy anatase lattice trapping sites (*i.e.*, synergistic effects),[29,30] these energetic mechanisms are strongly influenced by the local atomic environments, for example, cement nanoparticle grain boundaries, which are dictated by the cement composition. Other factors that are embedded in the cement composition are transition metals which may participate in redox reactions and thus interfere with photocatalysis.[16] In essence, in TiO_2−cement composites, the cement composition drives the dynamics of cement dissolution, crystal growth, and grain boundaries that in turn define the microstructure of the hydrated cement products engulfing TiO_2. As an example, SEM and WDS images (Figure 3) depict color mapping of the titanium distribution on the surface of the TiO_2−WPC composites, illustrating better dispersion of the photocatalyst on the WPC matrix amended with P25 than with anatase particles (Table 2), despite

https://doi.org/10.1021/acs.langmuir.1c00654
Langmuir 2021, 37, 5699−5706

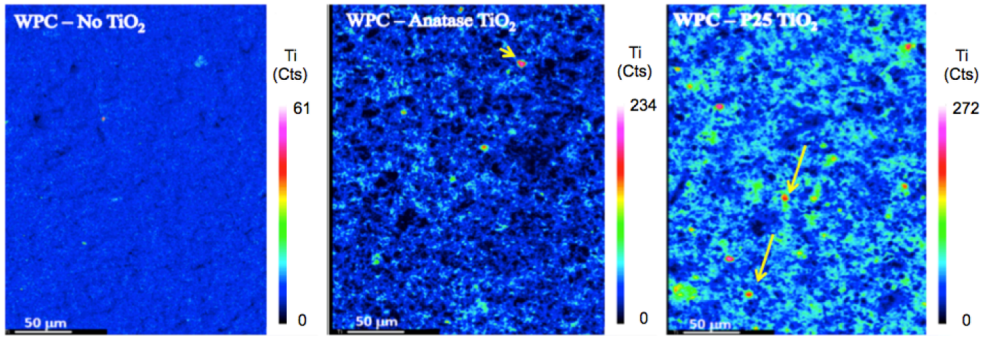

Figure 3. SEM/WDS images of titanium distribution on the surfaces of WPC composite plates. The arrows point to localized highest concentrations of TiO_2 according to the color scales (right of each image) based on X-ray counts (Cts) by the WDS detector. Accelerating voltage was set at 20.0 kV.

identical thorough mixing of both types of TiO_2 before cement hydration. Thus, the type of TiO_2 used (both crystal structure and size) is also an influential factor. However, considering all observations, including the lack of positive response of OPC, the role of cement composition appears to be far more influential on the overall photocatalytic water treatment efficiency.

Control cement plates (without added TiO_2) exhibited intrinsic photocatalytic activity (corrected for sorption) for MO removal, ranging from 13.8% in OPC to 16.9% in PPC (Figure 1). These performance differences can also be attributed to variations in cement composition (Table 1), which were investigated below *via* detailed combinatorial analysis.

Photocatalytic Degradation of 1,4-Dioxane. We selected WPC and OPC amended with P25 $nTiO_2$ to assess their efficiency for the removal of 1,4-dioxane (Figure 4). A positive control, commercial PHC, was used for benchmarking. WPC−P25 composites showed significantly higher (81.6%) 1,4-dioxane removal efficiency after 30 min of light irradiation (excluding sorption) compared to OPC−P25 (39.8%). Given the identical photocatalysts and testing conditions, this difference is attributed to the cement type composition and/

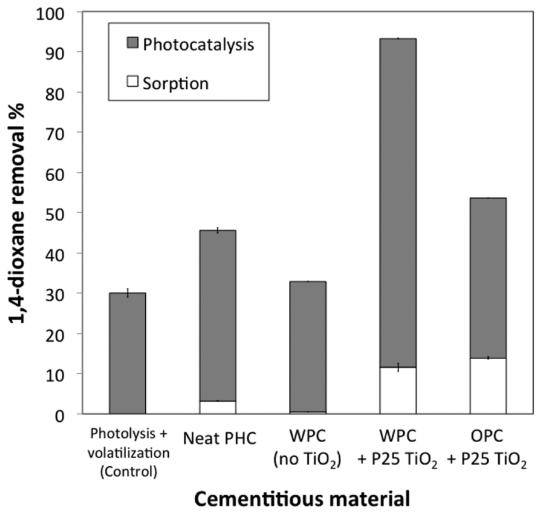

Figure 4. Differences in the removal of 1,4-dioxane by photocatalytic degradation and sorption. Error bars represent ± 1 standard deviation from the mean of all measurements. Test conditions were as follows: n = 3, exposure time: 30 min, initial pollutant concentration: 1 mg/L, λ = 254 nm, light intensity: 2.7 ± 0.4 mW/cm^2.

or microstructure. Comparing WPC and WPC−P25 in Figure 4, P25−WPC showed much higher 1,4-dioxane removal. PHC showed only about 9% net 1,4-dioxane removal efficiency after 30 min of irradiation.

TiO_2 leaching into treated water was also investigated using an inductively coupled plasma−optical emission spectrometer (ICP−OES) (Optima 4300 DV, PerkinElmer, USA). Prior to ICP−OES analysis, the samples were acid digested (mixing 5 mL sample aliquot with 4 mL of hydrofluoric acid and 8 mL of sulfuric acid and further diluting to 50 mL with 2% nitric acid). This analysis detected minimum Ti leaching from the photocatalytic composites into the water (detection limit 27 μg/L) at levels consistently lower than the recommended maximum Ti concentration in drinking water of 100 μg/L.[31]

Combinatorial Analysis of Cement Composition Versus Photocatalytic Treatment Performance. It is important to understand and decouple the inter-related role of individual cement components on the treatment efficiencies of TiO_2−cement composites. The various initial cement components first influence the hydrated phases of the cement and subsequently influence a myriad of properties such as density, porosity, pore size, pore size distribution, surface toughness, and coefficient of thermal expansion, which in turn influence the impurity removal performance. However, our aim is to bypass the study of such intermediate mechanisms and search for evident patterns that we can precisely control and directly link specific initial components to the removal efficiency. Once such patterns are identified, the mechanisms that drive them can be studied. To this end, we performed rigorous combinatorial analyses, including thousands of regressions on cement composition data, and measured removal efficiencies (Table S1). Such an exhaustive regression strategy was used because we had only a few, sparse compositional data (four averaged data points as illustrated in Table S1) for each photocatalytic efficiency test; hence fitting could be done with several possible functions, which were carefully filtered as follows. We considered 7806 combinatorial composite functions, each as a product of a few basic functions (x, $\sqrt{x}$, x^2, $1/x$, $\frac{1}{\sqrt{x}}$, and $1/x^2$) of initial cement phases, so that the cross-effects of multiple compositional phases can be captured (Figure 5 and Supporting Information). As composite functions such as the alite−belite ratio are already known to influence strength, we looked for similar functions that significantly correlate with pollutant removal performance. While the alite−belite ratio contains information of two phases (alite and belite), the functions we

https://doi.org/10.1021/acs.langmuir.1c00654
Langmuir 2021, 37, 5699−5706

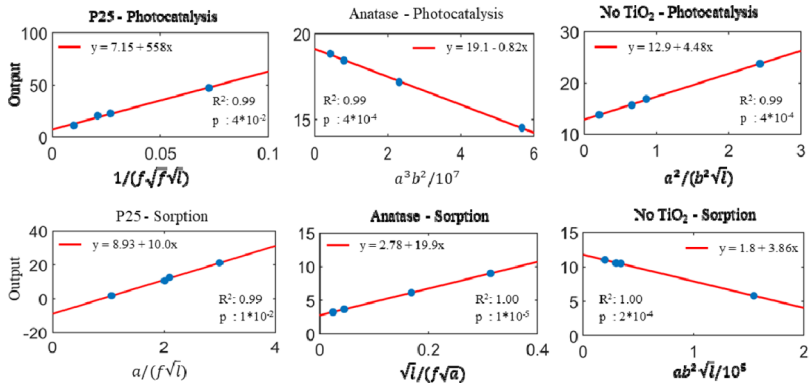

Figure 5. Regression plots of representative best-correlated composite functions. Output is the removal efficiency in %.

considered contain up to three phases, resulting in a wider search to uncover obscure but relevant influences. Given the relatively low number of data points, nonlinear composite functions may provide good fitting, but they may be nonunique and misleading. On the other hand, when composite functions of lesser nonlinearity are used, a reliable regression fit with good probability value, for example, $p < 0.05$, may not be achieved. To address this issue, we extracted important information from a set of all well-correlated composite functions (for which $R^2 > 0.98$ and $p < 0.05$) by observing repeating factors and trends. Table S2 shows representative well-correlated composite functions. For example, among the 50 well-correlated functions in the "anatase—photocatalysis" case, ferrite is a highly repeating factor appearing in 36 of them, and the direct functions of ferrite (*e.g.*, f, $\sqrt{f}$, and f^2) occur with a negative correlation coefficient with removal efficiency, while the inverse functions of ferrite (*e.g.*, $1/f$, $\frac{1}{\sqrt{f}}$, and $1/f^2$) occur with a positive coefficient. This is a clear indication that the photocatalytic performance of OPC, WPC, PPC, and PPC-2 was negatively correlated with their ferrite content. This finding is consistent with previous reports of deleterious effect of ferrite-related cement components such as Fe_2O_3 on photocatalytic NOx removal from air.[16]

In order to capture, abstract, and quantify all such repeating factors and trends, we defined a "correlation score" for each variable. This score is the difference between the percentage of well-correlated functions in which the variable appears with a positive correlation and the percentage in which it appears with a negative correlation. For example, in the case of "anatase—photocatalysis," ferrite appeared in ∼4% (2 out of 50) of the well-correlated composite functions with a positive correlation and ∼68% (34 out of 50) with a negative correlation; thus its correlation score becomes −64%. The rest of the well-correlated functions did not have ferrite. Table 3 summarizes all correlation scores for all variables in all cases (with individual plots shown in Figures S1−S3). The magnitude of the correlation score indicates how significant is the variable statistically in driving the output, while the sign of the score indicates its positive/negative correlation. Correlation scores with high magnitudes (>50%) indicate that this variable is a reasonably consistent driver of the output. In certain examples such as ferrite in the anatase-sorption case, the magnitude is as high as 91, showing clear evidence of inter-relation between the component and the impurity removal efficiency.

Based on this novel, comprehensive combinatorial analysis considering the photocatalytic cement composition and the measured treatment efficiencies (Figure 5, Tables S1 and S2) and the correlation scores (Table 3), we identified that the belite and ferrite components have strong inverse correlation with the photocatalytic removal efficiency. The effects of belite are the most consistent across all composites, irrespective of the type of TiO_2 added, closely followed by ferrite. Also, we observe that in many well-correlated functions, these two factors appear together. Therefore, in certain cases, even if one factor has a smaller score (such as belite in anatase-sorption), the other factor has a high score. Two other minor trends can also be observed in Table 3, namely, Al_2O_3 having negative correlation in the P25 composites and the expected positive effect of the natural content of rutile TiO_2 in cement in cases where there is no added TiO_2.[32] The underpinnings of the role of components such as belite and ferrite are complex and influenced by the resultant grain boundaries of cement hydration (microstructure, distribution, *etc.*) and their local electronic interactions with TiO_2, as described above. Although all combinatorial analyses were performed for MO removal by the photocatalytic composites, the above key findings are also valid for 1,4-dioxane removal. For instance, the higher 1,4-dioxane removal of WPC−P25 versus OPC−P25 is due to the lower belite, ferrite, and Al_2O_3 contents in WPC. This suggests the generality of our results and the robustness of our novel statistical approach. Broadly, this newly developed combinatorial computational method geared toward sparse experimental data can go beyond cement and photocatalysis, providing a robust statistical/screening tool for identifying influential compositional parameters and their overall effects when experimental performance data are limited.

Considering the engineering challenge posed at the beginning of this paper, even with these limited data, our quantitative statistical results now allow us to discard inefficient commercial cement formulations and/or to devise useful engineering strategies to turn OPC to photoactive

Table 3. Correlation Scores (%)

Output case	Alite	Belite	Calcite	Ferrite	Rutile	Al_2O_3
P25 - Photocatalysis	-33	-67	17	-50	0	-50
P25 - Sorption	50	-50	50	-50	0	-50
Anatase - Photocatalysis	-37	-77	-3	-64	8	-19
Anatase - Sorption	25	-28	-2	-91	-5	24
No TiO_2 - Photocatalysis	18	-51	-41	22	38	0
No TiO_2 - Sorption	-15	-46	-34	-27	65	-33

https://doi.org/10.1021/acs.langmuir.1c00654
Langmuir 2021, 37, 5699−5706

materials for water treatment. This is one of the key contributions of this paper, which provides *de novo* concepts and strategies for effective photocatalytic activity at scale. For example, one strategy can be reducing the ferrite content, which is a noncritical cement component for mechanical purposes but of great importance for photocatalytic activity, as demonstrated in this work. This slight composition optimization can satisfy both mechanical and photocatalytic functionalities of the cement composites, hence providing multifunctional infrastructure materials. In the next section, we discuss aging effect and regeneration treatment, which are two other important considerations to assess the longevity of photocatalytic cements.

Photocatalytic Generation of •OH by TiO_2–Cement Composites and Their Aging. Figure 6a shows the fluorescence emission spectra of 2-hydroxyterephthalate solutions after UVC irradiation on freshly regenerated cement plates. Both neat cement (unamended with TiO_2) and TiO_2–cement composites produced •OH, especially freshly regenerated WPC–P25 plates (Figure 6b). Composites with P25 generated approximately twice the amount of •OH compared to the neat samples and hence higher activity. In all these cases, the terephthalate ions readily react with the photogenerated •OH to make fluorescent 2-hydroxyterephthalate, which has an intense fluorescence emission band centered at 425 nm with an excitation wavelength of 315 nm (Figure 7).[33,34]

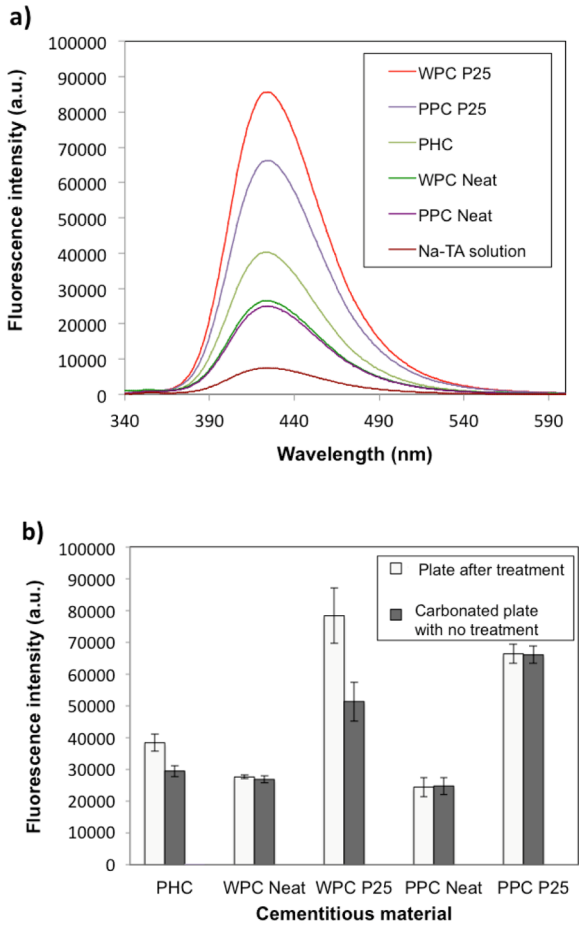

Figure 6. (a) Fluorescence spectra of 2-hydroxyterephthalate catalyzed by the cementitious plates and (b) influence of cement carbonation on the production of •OH by different photocatalytic cement formulations before (black columns) and after mechanical erosion and UV–H_2O treatment (white columns). Error bars represent ± 1 standard deviation from the mean of triplicate measurements. Test conditions were as follows: n = 3, exposure time: 30 min, TiO_2 content: 5% w/w, λ = 254 nm, light intensity: 21,500 lux.

One-week aged plates generated less •OH than corresponding freshly regenerated plates (Figure 6b). WPC–P25 experienced the most aging, whereas all other plates exhibited a relatively slow aging effect. Lower photocatalytic activity was mainly due to deposition of calcium carbonate on the composite surfaces, which hinders •OH generation (Figures 8 and S4). This is in accordance with previous aging studies on the photocatalytic abatement of NOx pollutants from air.[35] Nevertheless, the passivating calcium carbonate deposits are easily removed by the described regeneration treatment, leveraging the durability of the photocatalytic cement for multiple reuses for water treatment. This implies potential broad applicability of TiO_2–cementitious composites as an efficient, reusable water treatment unit, which could be embedded within long-lasting concrete infrastructures.

CONCLUSIONS

Combinatorics and correlation analyses can aid material selection to optimize the formulation of photocatalytic cements that enable affordable water purification in many resource-limited areas. While the photocatalytic activity is dependent on the cement composition, types of TiO_2, and the resultant microstructure of the composites, we found that cement composition is the most influential factor. In particular, the composition of OPC per se may be incompatible with both P25 and anatase TiO_2, calling for not only avoidance of this commercial cement formulation for photocatalytic water treatment applications but also precise engineering of trace cement components that enable photocatalytic activity while maintaining mechanical functionality. To this end, we developed a new generic statistical method using combinatorial functions and correlation scores applied to limited, sparse experimental data. This novel analytical approach revealed that belite and ferrite have strong inverse correlation with the water treatment efficiency among the various cement constituents. These empirical relationships suggest the benefits of mineral analysis of commercially available cements prior to their selection (and to consider their manipulation) to optimize photocatalytic composite performance. Beyond cement and photocatalysis, our developed generic combinatorial method can be applied to several other environmental problems to find meaningful performance trends when data are limited.

Compared to anatase, composites with P25 generated more •OH radicals, in agreement with their improved photocatalytic performance. Although aging initiated by precipitation of calcium carbonate slowed down the generation of •OH radicals, our proposed wet-rubbing method is a facile regenerative treatment strategy to restore photocatalytic activity and enable reuse for water treatment. Finally, while we inferred importance of cement composition and microstructure (*e.g.*, TiO_2 distribution, grain boundary, redox-active elements, *etc.*), future research is needed to fully understand the specific effects of microstructural parameters and their interactive effects with influential cement constituents, including other minor components, (*e.g.*, gypsum) to ensure efficient photocatalytic treatment. Overall, this work provides several new insights and quantitative metrics that can aid in the

https://doi.org/10.1021/acs.langmuir.1c00654
Langmuir 2021, 37, 5699–5706

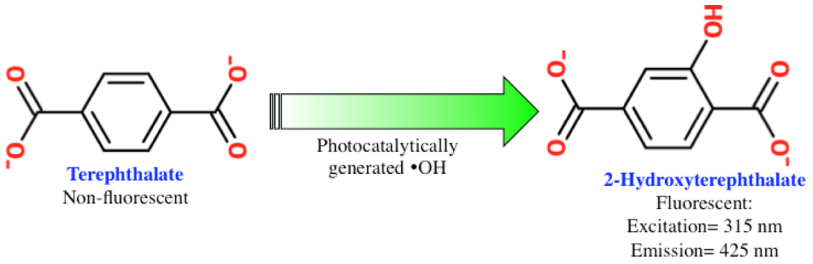

Figure 7. Reaction of terephthalate with the photocatalytically generated •OH to form fluorescent 2-hydroxyterephthalate.

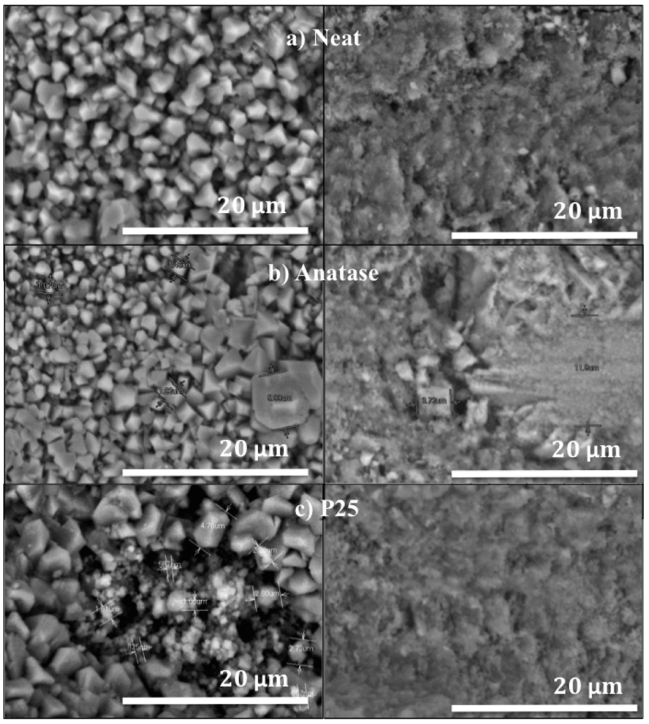

Figure 8. Calcium carbonate formation on WPC cement plates. Left panel shows SEM image after three reuse cycles under batch conditions. Right panel shows the same material after regeneration treatment (sanding off) of the cement surface.

selection and formulation of cementitious materials and pave the path toward science-based application of photocatalytically active cementitious composites for water purification.

■ ASSOCIATED CONTENT

Supporting Information

The Supporting Information is available free of charge at https://pubs.acs.org/doi/10.1021/acs.langmuir.1c00654.

Detailed statistical analysis, combinatorial composite functions, and XRD data (PDF)

■ AUTHOR INFORMATION

Corresponding Authors

Pedro J. J. Alvarez − *NSF ERC for Nanotechnology Enabled Water Treatment (NEWT), Rice University, Houston, Texas 77005, United States; Dept. of Civil and Environmental Engineering, Rice University, Houston, Texas 77005, United States;* orcid.org/0000-0002-6725-7199; Email: alvarez@rice.edu

Rouzbeh Shahsavari − *C-Crete Technologies, Stafford, Texas 7477, United States*; Email: rouzbeh@ccretetech.com

Authors

Pamela Zuniga Fallas − *NSF ERC for Nanotechnology Enabled Water Treatment (NEWT), Rice University, Houston, Texas 77005, United States; Dept. of Civil and Environmental Engineering, Rice University, Houston, Texas 77005, United States*

Jaime Quesada Kimzey − *Escuela de Química, Instituto Tecnológico de Costa Rica, Cartago 159-7050, Costa Rica*

Prabhas Hundi − *Dept. of Civil and Environmental Engineering, Rice University, Houston, Texas 77005, United States*

Md Tariqul Islam − *NSF ERC for Nanotechnology Enabled Water Treatment (NEWT), Rice University, Houston, Texas 77005, United States; Dept. of Chemistry, University of Texas, El Paso, El Paso, Texas 79968, United States;* orcid.org/0000-0001-5335-7239

Juan C. Noveron − *NSF ERC for Nanotechnology Enabled Water Treatment (NEWT), Rice University, Houston, Texas 77005, United States; Dept. of Chemistry, University of Texas, El Paso, El Paso, Texas 79968, United States;* orcid.org/0000-0002-2762-7802

Complete contact information is available at: https://pubs.acs.org/10.1021/acs.langmuir.1c00654

Notes

The authors declare the following competing financial interest(s): R.S. has a pending patent on cement formulation optimization, and computational and analytical component of this research.

■ ACKNOWLEDGMENTS

This research is supported by the NSF ERC on Nanotechnology-Enabled Water Treatment (EEC-1449500) and financial support of C-Crete Technologies LLC. We thank Sergi Garcia-Segura and Francesco Rossi for helpful discussions and Cory Schwarz and Jianhua Li for technical support with GC/MS and XRD, respectively. Fundación Technoinnovation subsidized PZ and Vicerrectoría de Investigación at ITCR subsidized JQ.

■ REFERENCES

(1) Diebold, U. The surface science of titanium dioxide. *Surf. Sci. Rep.* **2003**, *48*, 53−229.

(2) Baruah, S.; Najam Khan, M.; Dutta, J. Perspectives and applications of nanotechnology in water treatment. *Environ. Chem. Lett.* **2016**, *14*, 1−14.

(3) Lee, S.-Y.; Park, S.-J. TiO2 photocatalyst for water treatment applications. *J. Ind. Eng. Chem.* **2013**, *19*, 1761−1769.

(4) Cates, E. L. Photocatalytic Water Treatment: So Where Are We Going with This? *Environ. Sci. Technol.* **2017**, *51*, 757−758.

(5) Shan, A. Y.; Ghazi, T. I. M.; Rashid, S. A. Immobilisation of titanium dioxide onto supporting materials in heterogeneous photocatalysis: A review. *Appl. Catal., A* **2010**, *389*, 1.
(6) Singh, S.; Mahalingam, H.; Singh, P. K. Polymer-supported titanium dioxide photocatalysts for environmental remediation: A review. *Appl. Catal., A* **2013**, *462*, 178.
(7) Srikanth, B.; Goutham, R.; Badri Narayan, R.; Ramprasath, A.; Gopinath, K. P.; Sankaranarayanan, A. R. Recent advancements in supporting materials for immobilised photocatalytic applications in waste water treatment. *J. Environ. Manag.* **2017**, *200*, 60−78.
(8) Moghaddam, S. E.; Hejazi, V.; Hwang, S. H.; Sreenivasan, S.; Miller, J.; Shi, B.; et al. Morphogenesis of cement hydrate. *J. Mater. Chem. A* **2017**, *5*, 3798−3811.
(9) Jayapalan, A. R.; Lee, B. Y.; Fredrich, S. M.; Kurtis, K. E. Influence of Additions of Anatase TiO2 Nanoparticles on Early-Age Properties of Cement-Based Materials. *Transport. Res. Rec.* **2010**, *2141*, 41−46.
(10) Nazari, A.; Riahi, S. The effects of TiO2 nanoparticles on properties of binary blended concrete. *J. Compos. Mater.* **2011**, *45*, 1181−1188.
(11) Lee, B. Y.; Kurtis, K. E. Influence of TiO2 nanoparticles on early C3S hydration. *J. Am. Ceram. Soc.* **2010**, *93*, 3399−3405.
(12) Ma, B.; Li, H.; Mei, J.; Li, X.; Chen, F. Effects of nano-TiO2 on the toughness and durability of cement-based material. *Adv. Mater. Sci. Eng.* **2015**, *2015*, 583106.
(13) Bossa, N.; Chaurand, P.; Levard, C.; Borschneck, D.; Miche, H.; Vicente, J.; et al. Environmental exposure to TiO2nanomaterials incorporated in building material. *Environ. Pollut.* **2017**, *220*, 1160−1170.
(14) Demeestere, K.; Dewulf, J.; De Witte, B.; Beeldens, A.; Van Langenhove, H. Heterogeneous photocatalytic removal of toluene from air on building materials enriched with TiO2. *Build. Environ.* **2008**, *43*, 406−414.
(15) Folli, A.; Pade, C.; Hansen, T. B.; De Marco, T.; MacPhee, D. E. TiO2 photocatalysis in cementitious systems: Insights into self-cleaning and depollution chemistry. *Cem. Concr. Res.* **2012**, *42*, 539−548.
(16) Guo, M.-Z.; Poon, C. S. Superior photocatalytic NOx removal of cementitious materials prepared with white cement over ordinary Portland cement and the underlying mechanisms. *Cem. Concr. Compos.* **2018**, *90*, 42−49.
(17) Khataee, A. R.; Amani-Ghadim, A. R.; Rastegar Farajzade, M.; Valinazhad Ourang, O. Photocatalytic activity of nanostructured TiO2-modified white cement. *J. Exp. Nanosci.* **2011**, *6*, 138−148.
(18) Feng, S.; Song, J.; Liu, F.; Fu, X.; Guo, H.; Zhu, J. Chemosphere Photocatalytic properties , mechanical strength and durability of TiO 2/cement composites prepared by a spraying method for removal of organic pollutants. *Chemosphere* **2020**, *254*, 126813.
(19) Adamson, D. T.; Piña, E. A.; Cartwright, A. E.; Rauch, S. R.; Hunter Anderson, R.; Mohr, T.; et al. 1,4-Dioxane drinking water occurrence data from the third unregulated contaminant monitoring rule. *Sci. Total Environ.* **2017**, *596−597*, 236.
(20) Karges, U.; Becker, J.; Püttmann, W. 1,4-Dioxane pollution at contaminated groundwater sites in western Germany and its distribution within a TCE plume. *Sci. Total Environ.* **2018**, *619−620*, 712.
(21) Kano, H.; Umeda, Y.; Kasai, T.; Sasaki, T.; Matsumoto, M.; Yamazaki, K.; et al. Carcinogenicity studies of 1,4-dioxane administered in drinking-water to rats and mice for 2 years. *Food Chem. Toxicol.* **2009**, *47*, 2776−2784.
(22) Beranek, R. (Photo)electrochemical methods for the determination of the band edge positions of TiO 2-based nanomaterials. *Adv. Phys. Chem.* **2011**, *2011*, 786759.
(23) Zhang, Z.; Chuang, Y.-H.; Szczuka, A.; Ishida, K. P.; Roback, S.; Plumlee, M. H.; et al. Pilot-scale evaluation of oxidant speciation , 1 , 4-dioxane degradation and disinfection byproduct formation during UV / hydrogen peroxide , UV / free chlorine and UV / chloramines advanced oxidation process treatment for potable reuse. *Water Res.* **2019**, *164*, 114939.
(24) Zangeneh, H.; Zinatizadeh, A. A. L.; Habibi, M.; Akia, M.; Hasnain Isa, M. Photocatalytic oxidation of organic dyes and pollutants in wastewater using different modified titanium dioxides: A comparative review. *J. Ind. Eng. Chem.* **2015**, *26*, 1.
(25) Li, M.; Conlon, P.; Fiorenza, S.; Vitale, R. J.; Alvarez, P. J. J. Water level monitoring pressure transducers : a need for industry-wide standards. *Ground Water Monit. Remed.* **2011**, *31*, 70−76.
(26) Ishibashi, K.-i.; Fujishima, A.; Watanabe, T.; Hashimoto, K. Detection of active oxidative species in TiO2 photocatalysis using the fluorescence technique. *Electrochem. Commun.* **2000**, *2*, 207−210.
(27) Amen, D. K. H. Degree of Hydration and Strength Development of Low Water-to-Cement Ratios in Silica Fume Cement System. *Int. J. Civ. Environ. Eng.* **2011**, *1110*−15.
(28) Shetty, M. S. *Concrete Technology Theory and Practice*, Revised ed.; S Chand and Company Ltd.: New Delhi, 2005.
(29) Hurum, D. C.; Agrios, A. G.; Gray, K. A.; Rajh, T.; Thurnauer, M. C. Explaining the Enhanced Photocatalytic Activity of Degussa P25 Mixed-Phase TiO $_2$ Using EPR. *J. Phys. Chem. B* **2003**, *107*, 4545−4549.
(30) Su, R.; Bechstein, R.; Sø, L.; Vang, R. T.; Sillassen, M.; Esbjörnsson, B.; et al. How the Anatase-to-Rutile Ratio Influences the Photoreactivity of TiO2. *J. Phys. Chem. C* **2011**, *115*, 24287−24292.
(31) Dong, S.; Chen, C.; Li, D.; Sun, Y. A study of hygienic standard for titanium in the source of drinking water. *Chin. J. Prev. Med.* **1993**, *27*, 26−28.
(32) Stebbins, J. F. Aluminum Substitution in Rutile Titanium Dioxide: New Constraints from High-Resolution 27Al NMR. *Chem. Mater.* **2007**, *19*, 1862.
(33) Nakabayashi, Y.; Nosaka, Y. The pH dependence of OH radical formation in photo- electrochemical water oxidation with rutile TiO2 single crystals. *Phys. Chem. Chem. Phys.* **2015**, *17*, 30570−30576.
(34) Islam, M. T.; Jing, H.; Yang, T.; Zubia, E.; Goos, A. G.; Bernal, R. A.; et al. Fullerene stabilized gold nanoparticles supported on titanium dioxide for enhanced photocatalytic degradation of methyl orange and catalytic reduction of 4-nitrophenol. *J. Environ. Chem. Eng.* **2018**, *6*, 3827−3836.
(35) Chen, J.; Poon, C.-s. Photocatalytic cementitious materials: Influence of the microstructure of cement paste on photocatalytic pollution degradation. *Environ. Sci. Technol.* **2009**, *43*, 8948−8952.

https://doi.org/10.1021/acs.langmuir.1c00654
Langmuir 2021, 37, 5699−5706